

Stimulated Raman Scattering, Cascade-into-Condensate and Acceleration of Large Relativistic Electromagnetic Solitons in Intense Laser Interaction with an Underdense Plasma

LI Baiwen^{1,2,3}, ISHIGURO Seiji^{1,2}, ŠKORIĆ Miloš M.⁴ and TAKAMARU Hisanori⁵

¹The Graduate University for Advanced Studies, Toki 509-5292, Japan

²National Institute for Fusion Science, Toki 509-5292, Japan

³Institute of Applied Physics and Computational Mathematics, Beijing 100088, P.R.China

⁴Vinča Institute of Nuclear Sciences, POB 522, Belgrade 11001, Serbia and Montenegro

⁵Chubu University, 1200 Matsumoto-cho, Aichi 487-8501, Japan

(Received: 9 December 2003 / Accepted: 16 March 2004)

Abstract

Stimulated Raman scattering and Cascade-into-Condensate mechanism induced by intense laser in underdense uniform plasmas are studied by particle simulations. Standing-, backward- and forward-accelerated relativistic electromagnetic (EM) solitons are observed after multiple interactions. Apart from the inhomogeneity of plasma density the soliton acceleration depends upon both the laser intensity and the plasma length. The backward and forward solitons are accelerated towards the plasma-vacuum interface radiating energy in the form of low-frequency EM bursts. The soliton frequency is about one-half of the unperturbed electron plasma frequency. The transverse electric, magnetic and electrostatic fields have half-, one- and one-cycle structure in space, respectively.

Keywords:

stimulated raman scattering, raman cascade, electromagnetic solitons, particle simulations

1. Introduction

Relativistic laser-plasma interactions is a source of various electronic instabilities [1,2]. When a relativistic laser light propagates in underdense plasma, electron parametric instabilities, such as, forward and backward stimulated Raman scattering (F-SRS/B-SRS), and relativistic modulational instability (RMI), can develop [3]. They do not appear isolated but are often interconnected. A nonlinear interplay between B-SRS and F-SRS produces a strong spatial modulation of the laser pulse and the cascade in its frequency spectrum. The continuing instability growth through SRS cascade downshifts the pulse frequency from the fundamental to the bottom of the light spectra. The spectra of F-SRS clearly reveal the Raman cascade containing the first anti-Stokes, first-, second- and higher-order Stokes modes. It gets saturated by the photon condensation mechanism, related to strong depletion and possible break-up of the laser beam. In the final stage of the cascade-into-condensate mechanism, the depleted downshifted laser pulse gradually transforms into a train of ultra-short relativistic electromagnetic (EM) solitons [3].

Relativistic solitons are EM structure self-trapped by locally modified plasma refractive index through the relativistic electron mass increase and the electron density depletion by the ponderomotive force of an intense laser. They

are generated behind the front of the laser pulse and are made of nonlinear, spatially localized low-frequency EM fields. A fairly large part of the laser energy can be transformed into solitons. The generation and structure of EM solitons were analytically investigated and observed by particle simulation in intense laser interaction with underdense and overdense plasmas [4-6]. The solitons found in 1D and 2D particle simulations consist of slowly or non-propagating electron density cavities with EM field trapped inside and oscillate coherently with a frequency below the unperturbed plasma frequency and with the spatial structure corresponding to half a cycle (subcycle soliton) [5]. In a homogeneous plasma, solitons were found to exist for a long time, close to the regions where they were generated, and eventually decay by transforming the soliton energy into fast particles. In inhomogeneous plasmas, solitons move with the acceleration proportional to the density gradient toward the low density side. When a soliton reaches the plasma-vacuum interface, it radiates away its energy in the form of a short burst of low-frequency EM radiation [5,6].

In this paper, we present particle simulation results on SRS, cascade-into-condensate and large relativistic EM solitons created by linearly polarized intense laser in underdense homogeneous plasmas. We found that, in addition

to the plasma inhomogeneity, soliton acceleration is controlled by, both the laser intensity and the plasma length. In the rest, we just focus on the laser intensity effect. The frequency of the EM wave trapped inside the soliton is about one half of the unperturbed plasma frequency. The soliton electric field has the half-cycle structure in space, while the magnetic field and corresponding electrostatic (ES) field have the one-cycle structure.

2. Simulation model

One-dimension and three-velocity (1D3V) fully relativistic EM particle-in-cell (PIC) code is used. Simulation system length is $2700c/\omega_0$ in x direction, in this direction particles are allowed to move, where c and ω_0 are the vacuum speed of light and the laser frequency, respectively. Plasma length of $900c/\omega_0$ begins at $x = 0$ and ends at $900c/\omega_0$; in the front and rear side of the plasma there are two $900c/\omega_0$ long vacuum regions. Ions are kept immobile as a neutralizing background. The plasma density and its initial electron temperature are $n = 0.032n_{cr}$ and $T_e = 350$ eV, where $n_{cr} = \omega_0^2 m_e / 4\pi e^2$ is the critical density. The number of cells is 10 per $1c/\omega_0$ and 80 particles in each cell. Laser is linearly-polarized with the electric field E_0 along the y -direction and the normalized amplitude $\beta = eE_0/m_e\omega_0c$, where e and m_e are the electron mass and charge, respectively. The electrons which enter vacuum region build a potential barrier that prevents more electrons of leaving the plasma. For these electrons as well as for outgoing EM waves, two additional damping regions are used. The time, electric field and magnetic field are normalized to the laser period $2\pi/\omega_0$, $m_e\omega_0c/e$ and $m_e\omega_0/e$, respectively; the time is taken zero, $t = 0$, when the laser arrives at the vacuum-plasma boundary.

3. Stimulated Raman cascade and the photon condensation process

When intense laser propagates in underdense plasma, the first stage is dominated by B-SRS process; matching conditions $\omega_0 = \omega_s + \omega_{ek}$ and $k_0 = k_s + k_p$ are well-satisfied, where ω_0 , ω_s and ω_{ek} are the frequency of incident EM wave, scattered EM wave and electron plasma wave (EPW), while, k_0 , k_s and k_p are the corresponding wave number, respectively. For example, for laser amplitude $\beta = 0.3$, the dominant ES wave is excited EPW with frequency $\omega_{pe} = 0.18\omega_0$, and the corresponding backscattered Stokes wave with frequency $\omega_s = 0.82\omega_0$ (see Fig. 1). As time goes on, following the B-SRS, complex nonlinear processes involving F-SRS and RMI develop, such as, spectral cascade and broadening, which effectively transfer the laser pulse energy to higher order scattering modes. A nonlinear interplay between B-SRS and F-SRS produces a strong spatial modulation of the laser pulse and the down cascade in its frequency spectrum. Along the propagation beam, there is typically the Raman cascade in the light spectrum from fundamental laser frequency toward lower frequencies. The first Stokes line is significant, further along the propagation, the Stokes mode becomes a new pump, which decays via a secondary Raman scattering, and so on.

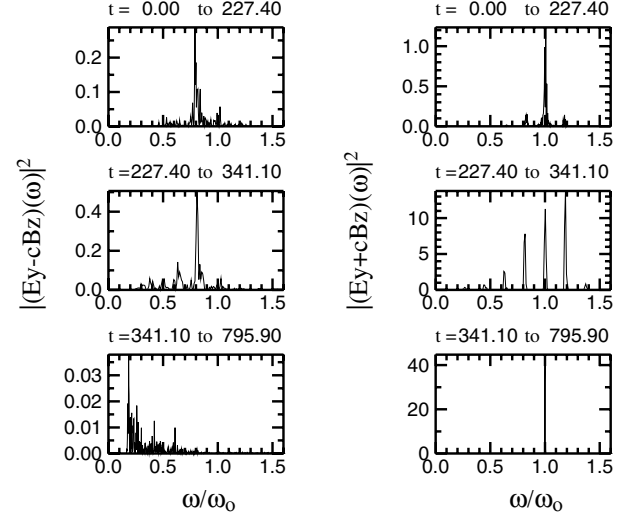


Fig. 1 Spectra (a.u.) of reflected (left) and transmitted (right) EM waves for $\beta = 0.3$.

As shown in Fig. 1, the continuing instability growth through stimulated Raman cascade downshifts the frequency spectrum from the fundamental to close to the perturbed electron plasma frequency. The spectrum of the F-SRS clearly reveals the linear Raman cascade containing not only the first anti-Stokes mode, but also the first-, second- and higher-order Stokes modes. Parametric down-cascade of the laser pulse into the higher-order B-SRS and F-SRS harmonics saturates into the Photon Condensate at the bottom of the light spectrum, related to strong depletion and possible break-up of the laser beam and relativistic electron heating [4]. The process is eventually halted below the plasma frequency, which is the cutoff for a laser propagation.

4. Acceleration of large amplitude relativistic electromagnetic solitons

For the laser amplitude, $\beta = 0.3$ case, when SRS through cascade-into-condensate is saturated, as shown in Fig. 2; a spatially localized, non-propagating electron density cavity is created. Inside, the EM field is trapped and oscillates coherently; that is, a large amplitude localized standing relativistic EM soliton comes into form. In Fig. 3 (top), the frequency spectra of EM and ES waves trapped inside the soliton region are plotted. In addition to the laser fundamental and the excited perturbed EPW, EM component with the frequency close to $0.13\omega_0$, and corresponding ES component with the frequency near to $0.87\omega_0$ are observed, one can see this phenomenon roughly as a 3-wave resonant coupling. The size of the soliton is about $5\lambda_0$ (λ_0 is laser wavelength in vacuum), close to the electron plasma wavelength λ_p [5]. Fig. 3 shows the structure of the soliton, ES field E_x (averaged over λ_p) is the one-cycle structure, and the corresponding transverse electric field E_y (averaged over λ_0) is the half-cycle structure and the magnetic field B_z is the one-cycle structure. The spatial EM structure is oscillatory in time, but the ES structure is not. The explanation comes directly from Maxwell's equations. The Faraday law gives $B_z \sim \partial E_y / \partial x$; indeed, the x -

derivative of the Gaussian soliton profile E_y , gives B_z in Fig. 3. Similarly, from the Poisson equation, integration over $-x$ of the Gaussian density cavity (Fig. 2) leads to the ES field E_x in Fig. 3. Moreover, PIC data and analytics e.g. eqs. (4)–(7) of [6], show that zero-harmonic term dominates the electron density perturbation (ponderomotive term). Therefore, the

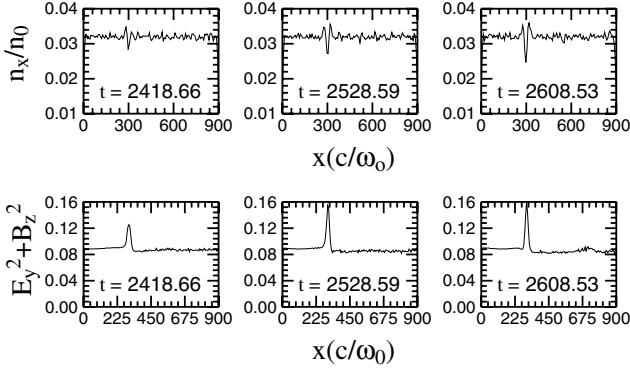


Fig. 2 Plasma density n/n_0 and EM energy density $E_y^2 + B_z^2$ snapshots (averaged over λ_0) for laser pulse, $\beta = 0.3$.

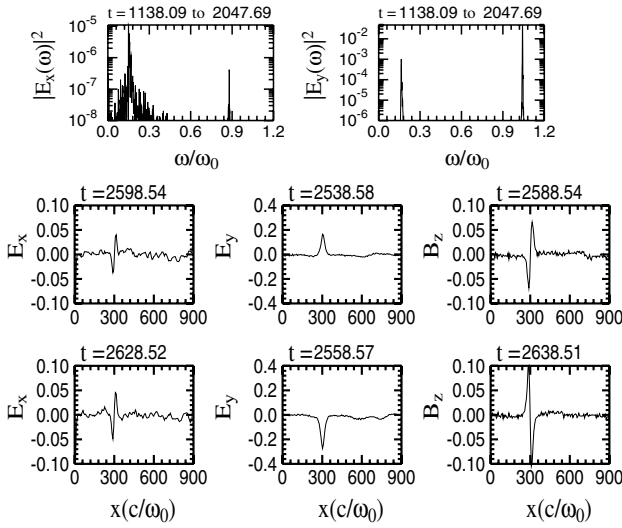


Fig. 3 Spectra (a.u.) of EM and ES waves inside the soliton, and profiles of ES field, E_x , transverse electric E_y and magnetic field B_z , for $\beta = 0.3$.

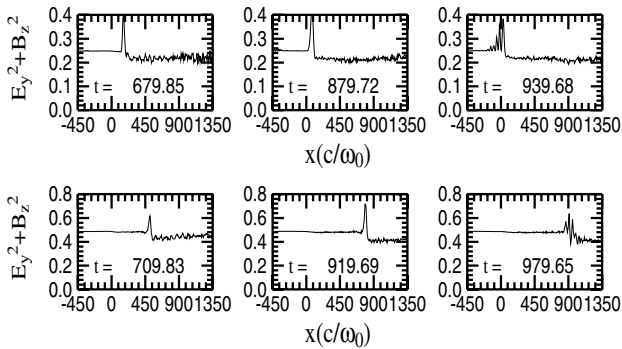


Fig. 4 The EM energy density $E_y^2 + B_z^2$ snapshots for $\beta = 0.5$ (top) and for $\beta = 0.7$ (bottom).

Poisson equation gives the corresponding non-oscillatory ES field, like E_x in Fig. 3.

However, by increasing the laser amplitude to $\beta = 0.5$, as shown in Fig. 4, the soliton dynamics appears different to that in the standing soliton $\beta = 0.3$ case. The observed, large localized EM soliton is backward-accelerated towards the plasma-vacuum interface, where it radiates its energy away in the form of low-frequency EM burst, due to a non-adiabatic interaction with the plasma boundary. As a result, one observes a very high transient reflectivity. As we further increase the amplitude to $\beta = 0.7$, as shown in Fig. 4, large localized EM soliton can be still detected. However, the interesting feature is that the soliton is now forward-accelerated. Again, the soliton at the plasma-vacuum (rear) interface irradiates its energy away in the form of low-frequency EM waves. During the solitary wave radiation very high transient transmittivity can be detected.

The frequency of backward and forward accelerated solitons was measured close to $0.5\omega_{pe}$; the size and the structure were similar to the standing soliton $\beta = 0.3$ case. Furthermore, the EM energy density profile shows that the front value is larger than at the rear side of the soliton; still, for large amplitudes, the difference is greater than that in the $\beta = 0.3$ case. The difference in EM energy appears to be mainly transferred to the soliton, also partly to other processes (e.g. heating). The steep EM energy gradient over the short transition layer of the soliton length (c/ω_p -classical skin depth) corresponds to the ponderomotive force acting on plasma electrons. The resulting acceleration will push the electron cavity with the soliton in the forward direction. Basically, the longitudinal electron motion is determined by the balance of the ES field and the ponderomotive force terms [6]. The large flow of relativistic electrons in forward direction due to SRS, which drives ES fields, gets compensated by a cold (bulk) return current which moves plasma electrons backwards. Possibly, this is why at moderate intensity solitons are found to move backwards. At larger amplitudes, the ponderomotive term prevails, the acceleration is reversed and solitons are pushed forwards.

5. Summary and conclusions

Our other results do not comply with some of the earlier explanations apart from the standing soliton case [5,6]. Solitons move with an acceleration proportional to the density gradient towards the low density side due to the inhomogeneity of plasma density [5]. However, we found that in underdense homogeneous plasmas, apart from standing solitons, by varying the laser intensity, we could also detect the backward and forward accelerated solitons. Different plasma length and laser amplitude can change the complex details of the relativistic laser-plasma interaction. For example, the SRS cascade, photon condensation, electron acceleration and heating, and so on; can largely affect the soliton formation, its structure, acceleration and dynamics. To our knowledge, our results on acceleration of large relativistic EM solitons in the underdense homogeneous plasma layer

have not been presented in the past theoretical and simulation studies [5]. Furthermore, despite a large number of earlier works, a clear interpretation of the nature of the acceleration of soliton in uniform plasmas appears to be lacking.

One of us (M.M.Š) acknowledges a partial support of the Ministry of Science and Technologies of the Republic of Serbia, Project No. 1964. We thank Lj. Hadžievski for stimulating discussions.

References

- [1] D.W. Forslund *et al.*, *Phys. Fluids* **18**, 1002 (1975); *ibid.*, **18**, 1017 (1975).
- [2] K. Estabrook *et al.*, *Phys. Fluids* **26**, 1892 (1985); *ibid.*, **B 1**, 1282 (1989).
- [3] K. Mima *et al.*, *Phys. Plasmas* **8**, 2349 (2001); C. D. Decker *et al.*, *Phys. Rev. E* **50**, R3338 (1994).
- [4] R.N. Sudan *et al.*, *Phys. Plasmas* **4** (5), 1489 (1997); S. Poornakala *et al.*, *ibid.*, **9**, 1820 (2002); T. Zh. Esirkepov *et al.*, *JETP Lett.* **68**, 36 (1998).
- [5] S.V. Bulanov *et al.*, *Phys. Rev. Lett.* **82**, 3440 (1999); T. Esirkepov *et al.*, *ibid.*, **89**, 275002 (2003); Y. Sentoku *et al.*, *ibid.*, **83**, 3434 (1999).
- [6] Lj. Hadžievski, M.S. Jovanović, M.M. Škorić and K. Mima, *Phys. Plasmas* **9**, 2569 (2002).